Anatomy and Pathology/Oncology

Impact of Nintedanib and Anti-Angiogenic Agents on Uveal Melanoma Cell Behavior

Vera E. Pawlik, Svenja R. Sonntag, Salvatore Grisanti, Aysegül Tura, Vinodh Kakkassery, and Mahdy Ranjbar

Department of Ophthalmology, University of Lübeck, Lübeck, Germany

Correspondence: Vera E. Pawlik, Department of Ophthalmology, University of Lübeck, Lübeck 23562, Germany; vera.pawlik@uksh.de.

VK and MR authors contributed equally to this work and should be considered senior authors.

Received: June 30, 2023
Accepted: January 21, 2024
Published: February 21, 2024

Citation: Pawlik VE, Sonntag SR, Grisanti S, Tura A, Kakkassery V, Ranjbar M. Impact of nintedanib and anti-angiogenic agents on uveal melanoma cell behavior. *Invest Ophthalmol Vis Sci.* 2024;65(2):30. https://doi.org/10.1167/iovs.65.2.30

Purpose. The purpose of this study was to investigate the direct impact of the combined angiokinase inhibitor nintedanib as well as the anti-angiogenic agents ranibizumab, bevacizumab, and aflibercept on the primary uveal melanoma (UM) cell line Mel270 and liver metastasis UM cell line OMM2.5.

Methods. The metabolic activity, viability, and oxidative stress levels were analyzed by the Thiazolyl Blue Tetrazolium Bromide (MTT), LIVE/DEAD, and reactive oxygen species (ROS) assays. Expression of intracellular VEGF-A_{165} and VEGF receptor-2 was detected by immunofluorescent staining. The secretion of VEGF-A_{165} into the cell culture supernatants was evaluated by VEGF-A_{165} ELISA.

Results. Nintedanib, at a concentration of 1 µg/mL, resulted in a median reduction of metabolic activity (for Mel270 of approximately 38% and for OMM2.5 of 46% compared to the untreated control) without exerting toxicity in either cell line, whereas the other 3 substances did not result in any changes (which also means that none of the 4 substances led to an increased cell death). Moreover, nintedanib (1 µg/mL) induced oxidative stress in the Mel270 by approximately 1.2 to 1.5-fold compared to the untreated control, but not the OMM2.5 cells.

Conclusions. Nintedanib could suppress the growth of UM cells in a concentration-dependent manner. The metastatic UM cell line OMM2.5 was not sensitive to the pro-oxidant activity of nintedanib. This study was the first to investigate nintedanib in the context of UM. We propose further investigation of this substance to elucidate its effects on this tumor entity with the hope of identifying advantageous therapeutic options for future adjuvant tumor therapies.

Keywords: uveal melanoma (UM), nintedanib, in vitro, anti-VEGF, cell culture

Uveal melanoma (UM) is a rare entity of intraocular malignancy that develops from uveal melanocytes.[1] The incidence varies depending on the investigated population (between less than one to over 9 cases per million).[2,3] UM is a disease of elderly adults which peaks between 70 and 80 years of age.[4] There are several treatment options available, including radiotherapy,[5–7] surgical resection,[8] or the most radical approach of enucleation[9] or exenteration of the orbit.[10] These therapies target a local tumor control, which is often well achievable.[11] However, despite treatment, approximately half of the patients will develop metastases later in life,[12] with the liver as the main metastatic site.[13,14] Unfortunately, treating metastatic UM remains a significant challenge due to the lack of effective standard therapies and genetic heterogeneity between the different tumors of the individual patients. Patients with UM are often enrolled in traditional chemotherapy or clinical trials for cutaneous melanoma despite giving the fact that both tumor entities differ immensely[15] and therefore UM is known for not responding well to chemotherapy or immunotherapy like check point inhibitors, possibly, among others, due to its immunosuppressive microenvironment.[16] Latterly, since 2022, the US Food and Drug Administration (FDA) and the European Medicines Agency (EMA) approved the immunotherapeutic substance Tebentafusp, however, which was restricted to patients with UM characterized by HLA-A*02:01 positivity. It is known to be the first immunotherapy that provides significant survival advantages.[17]

The concept of anti-angiogenesis is a method of tumor therapy that has been established since the 1970s, yet its complexity is not fully understood.[18,19] Unfortunately, anti-angiogenic agents have shown limited success in previous clinical studies involving patients with UM. It is critical to consider the limitations of these previous clinical studies, including small cohorts, lack of randomization, non-placebo-controlled study design, and a mixing of patient populations between cutaneous melanoma and UM. However, some effects regarding the extension of stable disease were observed in certain cases.[20] Hence, there should be continued increase the focus on the cellular biological mechanisms of how such substances affect UM to better understand the reasons behind their efficacy or failure in lieu thereof. This approach should also involve the investigation of novel anti-angiogenic substances.

Investigative Ophthalmology & Visual Science

VEGF-A induced autocrine signaling was implicated in the malignant behavior of different tumor entities.[21–31] Possible effects relate to stimulation of VEGF-A secretion,[31] alteration of cell survival,[24,26,28] tumor cell invasiveness,[28] or migration,[32] or even resistance to chemotherapy.[27] However, previous studies have shown conflicting findings regarding the role of VEGF-A or its receptors in the growth of UM cells.[33–35] For instance, it was shown that the presence of UM itself could stimulate VEGF and its receptors in otherwise unaffected ocular tissue in a paracrine manner.[36] In addition, VEGF-A secretion was stimulated by hypoxic conditions in the UM cell lines Mel270 and OMM2.5.[37] Although the anti-VEGF antibody bevacizumab was able to slow down UM growth in a mouse model after intraperitoneal injection,[38] another study demonstrated the paradoxical growth of UM in mice under intravitreal bevacizumab therapy.[39] Likewise, the proliferation of the human melanoma cell lines Mel285 and OMM2.3 was reduced through bevacizumab, whereas the expression of VEGF-A mRNA was stimulated by bevacizumab under hypoxic conditions.[39] Additionally, in clinical practice, several case reports have documented instances where UM tumor growth was observed in patients following intravitreal administration of bevacizumab.[40,41] Conversely, intravitreal anti-VEGF therapy is routinely used for radiation-induced macular edema following UM irradiation.[42] This practice may warrant critical reconsideration in the future, depending on the evolving understanding of the underlying pathomechanisms.[39] These incongruent and to some extent contradictory findings illustrate the complexity of the VEGF-related signaling pathways in UM and the urgent need for further investigation.

Most UM cell lines express VEGF-A_{165} and other forms of pro-angiogenic factors, such as the basic fibroblast growth factor (FGF),[37,43–46] as opposed to the normal melanocytes.[44] Additionally, VEGF receptors have been detected in the cytosol of UM cells, suggesting that autocrine and paracrine signaling may occur.[37,46] Given that the development of UM metastasis can only occur hematogenously and UM is well vascularized,[33,47] the objective of this study was to investigate the direct impact of the anti-VEGF agents ranibizumab,[48] bevacizumab,[49] and aflibercept,[50] as well as the triple angiokinase inhibitor nintedanib, which can block the receptors of VEGF, FGF, and platelet-derived growth factor,[51–53] on the UM cells. The study design thus offers the opportunity to compare the cell behavior of primary tumor and metastasis. Additionally, it allows for a comparison among three ophthalmologically established substances and a new molecule that has not yet been explored in the field of ophthalmology, specifically in the context of UM. The rationale behind the use of nintedanib in this study was to investigate whether broad receptor inhibition could potentially have a stronger or different effect in the tumor cells compared to the other three tested substances, possibly through addressing overlapping signaling pathways.

Methods

Cell Lines and Culturing

The UM cell lines Mel270 and OMM2.5 were obtained from Professor Martine J. Jager (Leiden, The Netherlands). Mel270 is a UM cell line originating from the primary tumor, whereas OMM2.5 is established from a liver metastasis of the same patient with UM (additional information about the reasons for choosing the two cell lines are provided in the supplementary material).[54,55] This provided us with the opportunity to comparatively assess the behaviors of the primary tumor cell line and cells from a metastasis, as both tumor cell lines have been derived from the same patient, but on the other hand could presumably differ in behavior from each other due to evolutional changes in the cells during metastatic processes.[56,57] Cells were maintained in the complete culture medium which consisted of RPMI 1640 with 2 mM L-Glutamine (BioWhittaker; Lonza, Verviers, Belgium), 10% fetal bovine serum (FBS; Biochrom GmbH, Berlin, Germany), and 1% penicillin/streptomycin (Biochrom GmbH, Berlin, Germany),[58] whereas the serum-starved culture medium contained only 1% FBS.[59] After cultivation at 37°C and 5% CO_2 until predominant confluence, the culture was passaged for the performance of different assays.

The test substances included the VEGF-A inhibitors ranibizumab[48,60] (in concentrations of 62.5, 125, and 250 µg/mL; Novartis Pharma, Basel, Switzerland), bevacizumab[49,61] (125, 250, and 500 µg/mL; Hoffmann-La Roche AG, Basel, Switzerland), and aflibercept[50] (250, 500, and 1000 µg/mL; Bayer Vital GmbH, Leverkusen, Germany), as well as the multi-angiokinase inhibitor nintedanib[51–53] (0.001, 0.1, and 1 µg/mL; Selleck Chemicals LLC, Houston, TX, USA). The stock solution of nintedanib was prepared by dissolving in dimethylsulfoxide (DMSO; Sigma-Aldrich Chemie GmbH, Steinheim, Germany). As previously described,[62,63] the final concentration of DMSO, which ranged between 0.0005% and 0.05% (v/v) for 0.01 to 1 µg/mL nintedanib, respectively, was not considered to be interfering with the following experiments. Cells that were incubated in complete or serum-starved medium without the addition of test substances served as controls. Please note that additional concentrations were tested for Thiazolyl Blue Tetrazolium Bromide (MTT) assay (see below).

Thiazolyl Blue Tetrazolium Bromide Assay

Cells were seeded into microtiter plates (Life Sciences, Corning, NY, USA) at a concentration of 5×10^3 cells/100 µL/well in full medium and allowed to attach overnight, followed by the incubation in fresh full medium with or without the test substances (at concentrations of 0.005, 0.01, 0.025, 0.05, 0.1, 0.25, 0.5, and 1 µg/mL for nintedanib and 1, 10, 50, 125, 250, 500, 750, and 1000 µg/mL for the other 3 substances) for 48 hours. The stock solution of MTT (5 mg/mL in PBS; Gibco by Lifetechnologies, Carlsbad, CA, USA) was added at a dilution of 1:5 (v/v) and the cells were incubated further for 3.5 hours.[64,65] Measurement of absorbance (UV/visual absorption spectroscopy in optical density [OD]) was performed using a spectrophotometer (Molecular Devices GmbH, Biberach an der Riss, Germany) at 570 nm[64] after dissolving the MTT crystals with DMSO.[66] Negative controls were performed by measuring wells without cells but with the addition of MTT solution to prevent false positive results.

Reactive Oxygen Species Assay

Cells were seeded into black microtiter plates (Thermo Fisher Scientific, Roskilde, Denmark) in full medium at a density of 5×10^5 cells/100 µL/well and allowed to attach overnight, followed by a change to serum-starved medium for another 24 hours and then incubation with the test

substances in fresh serum-starved medium for a further 24 and 48 hours. Reactive oxygen species (ROS) detection was performed by a fluorometric assay, as described by the manufacturer (Lifetechnologies, Eugene, OR, USA), which uses a fluorometer (SpectraMax i3x; Molecular Devices GmbH, Biberach an der Riss, Germany) at the wavelengths of 487 nm and 532 nm (relative fluorescence units [RFU]).[67] Blanks were measured from the cells that were incubated with the same substance concentrations but without adding the assay reagent. The blanks were later subtracted from the corresponding values to exclude the possible autofluorescence. In addition, at the beginning of the experiments, negative controls were performed without cells but with cell medium and ROS solution.

Live/Dead Assay

Cells were seeded into 8-well chamber slides (Thermo Scientific, Rochester, NY, USA) at a concentration of 100,000 cells/400 µL/well in full medium, allowed to attach overnight, followed by serum-starvation (1% FBS) for another 24 hours and incubated for 24 and 48 hours with the test substances that were diluted in fresh serum-starved medium. The fluorescent LIVE/DEAD Cell Imaging Assay (488/570 nm; Lifetechnologies, Eugene, OR, USA) was performed following the manufacturer's instructions.[68–71] Cells were visualized under 100x magnification using a fluorescent microscope (Leica DMI 6000B, Wetzlar, Germany) with a monochrome digital camera (DFC350FXR2; Leica) and the filter sets Cy5/Y3 (exposure time 1030 ms, intensity 3, and gain 6.1) and Alexa488/L5 (exposure time 545 ms, intensity 3, and gain 6.1). Negative controls were performed by microscoping chamber slides without addition of fluorescent solution.

Three digital images per well were randomly taken (Leica Application Suite Advanced Fluorescence software 2.7.0.9329), blinded, and quantified using the ImageJ software (National Institutes of Health, Bethesda, MD, USA).[72] Cell survival was calculated by building a quotient out of the area of living cells and the total cell area for each image.

Immunofluorescent Staining

UM cells were seeded, cultured, and incubated similarly to the LIVE/DEAD assay. After 24 or 48 hours of incubation, the cells were fixed with paraformaldehyde (4% in PBS; MERCK KGaA, Darmstadt, Germany), permeabilized with Triton X-100 (0.1% in PBS; Serva Electrophoresis GmbH, Heidelberg, Germany), and blocked for at least 30 minutes in normal goat serum (2% in PBS; Sigma-Aldrich, Millipore, Temecula, CA, USA). The anti-human primary antibodies against human VEGF-A_{165} (Human VEGFA PAb, polyclonal, IgG, rabbit; Thermo Scientific, Rockford, IL, USA) or VEGF receptor-2 (Pierce CD309 / VEGFR2 Antibody (4B4), monoclonal, IgG1, mouse; Thermo Scientific, Rockford, IL, USA) were diluted 1:300 in Tris-buffered saline with 0.1% bovine serum albumin. Cells were incubated with the primary antibodies overnight at 4°C, followed by the secondary antibodies goat anti-rabbit IgG (H+L) Alexa Fluor 488 (Millipore, Temecula, CA, USA; 1:400 in PBS) or goat anti-mouse IgG (H+L) DyLight 550 (Thermo Scientific, Rockford, IL, USA; 1:400 in PBS) for 1 hour at 37°C. Cell nuclei were counterstained with DAPI (0.001 µg/mL in PBS, Invitrogen by Thermo Fisher Scientific, Paisley, UK). Negative controls were performed by adding only the secondary antibody without the primary antibody.

Three images per well were randomly taken using the same microscope and camera as in the LIVE/DEAD assay under 400x magnification (DAPI/A4 with an exposure time of 100 ms, intensity 4, and gain 6.1; Alexa488/L5 with an exposure time of 2000 ms, intensity 5, and gain 6.1; Cy5/Y3 with an exposure time of 700 ms, intensity 4, and gain 6.1).

After blinding all images, semiquantitative measurement of positive stain was calculated using ImageJ. For each image, the positive fluorescent area for VEGF-A_{165} or VEGFR2 was divided through positive DAPI area and multiplied with cell count of each image, so that a value of mean expression for VEGF-A_{165} or VEGFR2 per cell was provided.

VEGF-A_{165} Enzyme-Linked Immunosorbent Assay

The supernatants of cells were collected after the incubation with or without the test substances for 24 hours. VEGF-A_{165} in the culture medium was detected by ELISA following the manufacturer's instructions and also negative controls were done according to these instructions (Thermo Scientific Pierce Biotechnology, Rockford, IL, USA).[73]

Statistical Analysis

Data were analyzed using the software Microsoft Excel (Microsoft Corporation, Redmond, WA, USA) as well as Graphpad Prism 7 and 8 (Graphpad Software, LLC, USA). Supplementary Table S1 gives an overview about the performed sample sizes, technical replicates, and repetition rates for each experiment. Values were normalized to the medians of the corresponding controls so that the results are shown as "percentage of control." Descriptive statistical analysis was done by calculating the median, interquartile range (IQR), minimum, and maximum for each group and presented as box-and-whisker plots. The comparison of two groups was performed by using the exact Mann Whitney U test. P values < 0.05 were considered as significant.

Results

Optimal Dosage of Nintedanib, Ranibizumab, Bevacizumab, and Aflibercept on the Mel270 and OMM2.5 Cells Based on the Metabolic Activity

The extent of metabolic activity was evaluated by the MTT test after the incubation of the Mel270 and OMM2.5 cells for 48 hours with or without the test substances in complete medium with 10% serum. Nintedanib was administered at the concentration range of 0.005 to 1 µg/mL whereas ranibizumab, bevacizumab, and aflibercept were provided at the doses between 1 and 1000 µg/mL.

In the Mel270 cells, the highest tested concentration of nintedanib (1 µg/mL) resulted in an approximately 38 or 45% decrease in the median metabolic activity compared to the untreated control or 0.5 µg/mL Nintedanib, respectively ($P < 0.001$ and $P = 0.002$, respectively; Fig. 1A). Incubating the Mel270 cells with ranibizumab (Fig. 1B), bevacizumab (Fig. 1C), or aflibercept (Fig. 1D) resulted in no concentration-dependent tendencies or differences compared to the control group.

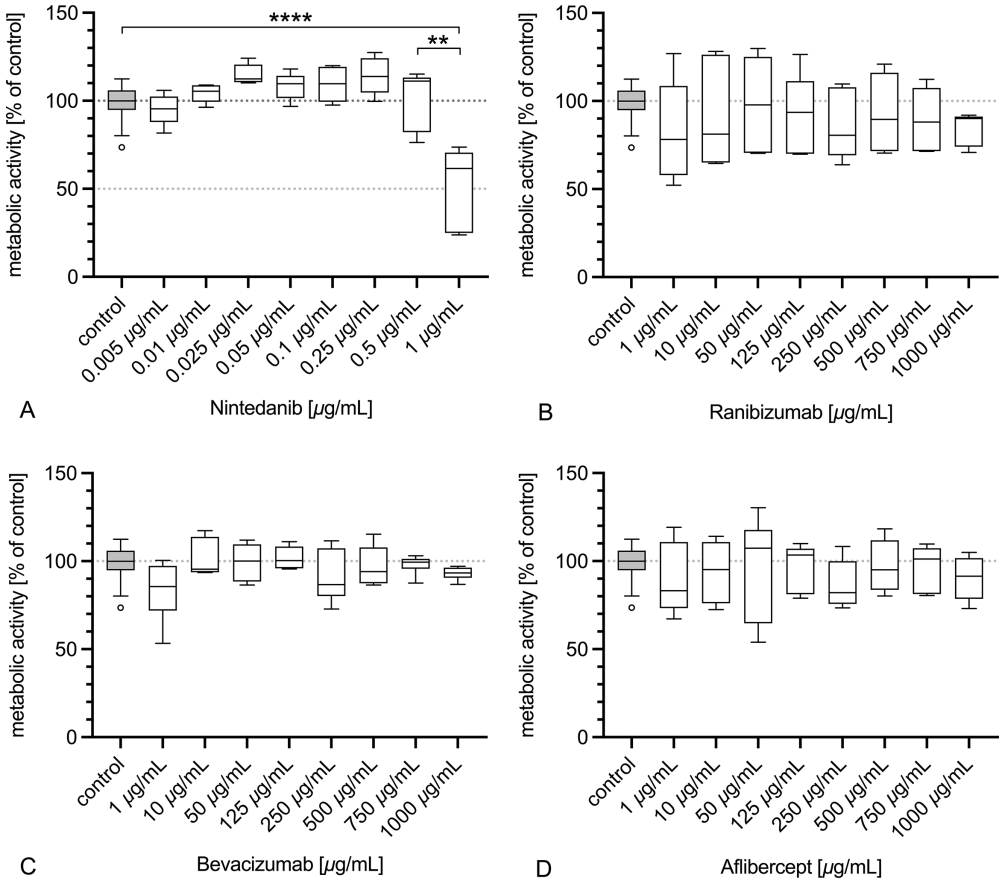

Figure 1. Metabolic activity of the cell line Mel270 as a percentage of untreated control as determined by the MTT assay after 48 hours of incubating the test substances. Cells were incubated in full medium with increasing concentrations of (**A**) nintedanib (0.005 to 1 µg/mL), (**B**) ranibizumab (1 to 1000 µg/mL), (**C**) bevacizumab (1 to 1000 µg/mL), and (**D**) aflibercept (1 to 1000 µg/mL; $n = 3$) for 48 hours. Absorption spectroscopy was taken in the unit (OD; optical density) at 570 nm. The results were normalized to the medians of the untreated controls of every repetition (n), respectively, and are therefore presented as the percentage of untreated control (%; lacking any unit). For the control group statistically simple outliers (degrees) were detected as shown in the figure, that represent values of more than 1.5-fold of the interquartile range in Tukey's box plots. None of the three different VEGF-A inhibitors had any impact on metabolic activity compared to the untreated control group, that also applies to the concentrations of nintedanib between 0.005 and 0.5 µg/mL. In contrast, the incubation with the highest concentration of nintedanib (1 µg/mL) decreased metabolic activity compared to the control ($P < 0.001$ ****) and in comparison to the lower tested concentrations of nintedanib ($P = 0.002$ **), as determined by the Mann Whitney U test.

The highest tested concentration of nintedanib (1 µg/mL) could also reduce the median metabolic activity of the OMM2.5 cells by approximately 46 or 52% compared to the control group and 0.5 µg/mL nintedanib, respectively ($P < 0.001$ and $P = 0.002$, respectively; Fig. 2A). For ranibizumab (Fig. 2B), bevacizumab (Fig. 2C), or aflibercept (Fig. 2D), there were neither concentration-dependent trends nor any indication of a difference compared to the control group.

Based on these findings, three concentrations of each substance were chosen for the subsequent experiments. The concentrations of ranibizumab, bevacizumab, and aflibercept were determined by considering their intraocular concentrations after a regular intravitreal injection, assuming a vitreous volume of 4 mL.[74,75] Specifically, ranibizumab was tested at the concentrations of 62.5, 125, and 250 µg/mL, bevacizumab at 125, 250, and 500 µg/mL, and aflibercept at 250, 500, and 1000 µg/mL. Intravitreous clinical doses resemble each medium dosage, flanked by halved and doubled concentrations. As no information was available for nintedanib's intraocular use, its concentrations were solely based on the results of the MTT assay, and the 3 concentrations of 0.01, 0.1, and 1 µg/mL were selected. This decision was also substantiated by the available pharmacological data for nintedanib on extraocular human cells.[51,76]

Viability and Toxicity in Response to the Test Substances

In the Mel270 cells, the LIVE/DEAD assay revealed no evidence of changes in viability after the 24- or 48-hour incubation with any of the test substances compared to the control group, with the percentage of viable cells being in a narrow range around 100% of the control (Figs. 3A, 3B, Supplementary Fig. S1).

In the OMM2.5 cells, the median viability values after the nintedanib treatment for 24 hours were also similar to the median of the control group, except for a slight reduction to 99% for 1 µg/mL Nintedanib, indicating lower cell survival in response to the highest concentration of this inhibitor ($P = 0.003$; Fig. 3C, see Supplementary Fig. S1). However, this effect could only become apparent graphically through the scaling of the ordinate (see Fig. 3C).

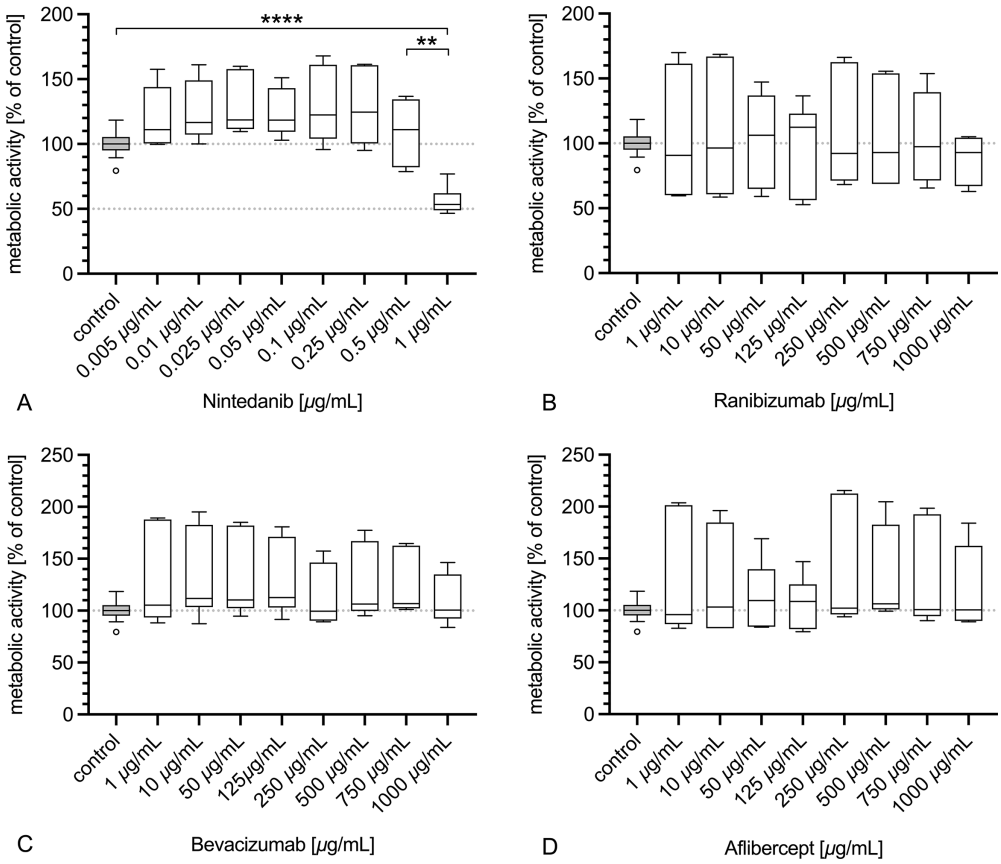

Figure 2. Metabolic activity of the cell line OMM2.5 as the percentage of untreated control as determined by the MTT assay after 48 hours of incubating the test substances. Cells were incubated in full medium with (**A**) nintedanib (0.005 to 1 µg/mL), (**B**) ranibizumab (1 to 1000 µg/mL), (**C**) bevacizumab (1 to 1000 µg/mL), and (**D**) aflibercept (1 to 1000 µg/mL) in increasing concentrations ($n = 3$) for 48 hours. Absorption spectroscopy was taken in the unit (OD; optical density) at 570 nm. The results were normalized to the medians of the untreated controls of every repetition (n), respectively, and are therefore presented as the percentage of untreated control (%; lacking any unit). For the control group, statistically simple outliers (degrees) were detected as shown in the figure, that represent values of more than 1.5-fold of the interquartile range in Tukey's box plots. Similar to the results for the cell line Mel270 (see Fig. 1), OMM2.5 also showed a lower metabolic activity in response to the highest concentration of nintedanib (1 µg/mL) compared to the untreated control group ($P < 0.001$ **** and $P = 0.002$ ** as determined by the Mann Whitney U test). Lower concentrations of nintedanib (0.005 to 0.05 µg/mL) as well as all concentration groups of the three substances ranibizumab, bevacizumab, and aflibercept (1 to 1000 µg/mL) did not result in any effects compared to the control. As opposed to the data of nintedanib, the remaining test substances did not indicate any effects on metabolic activity.

No difference in viability was detected after the 48-hour exposure of the OMM2.5 cells to nintedanib at any of the tested concentrations (Fig. 3D, Supplementary Fig. S1). Likewise, the incubation of the OMM2.5 cells with ranibizumab, bevacizumab, or aflibercept for 24 and 48 hours at the indicated concentrations did not influence the viability compared to the control (see Figs. 3C, 3D, Supplementary Fig. S1).

Oxidative Stress in Response to the Test Substances

Incubation of the Mel270 cells with 1 µg/mL of nintedanib for 24 hours resulted in an almost 1.5-fold increase in the accumulation of ROS compared to the control ($P < 0.001$) and a 1.2-fold elevation compared to the intermediate concentration of nintedanib at 0.1 µg/mL ($P = 0.002$; Fig. 4A). Similarly, the Mel270 cells that were incubated for 48 hours with 1 µg/mL nintedanib demonstrated 1.4-fold higher levels of oxidative stress compared to the control ($P = 0.01$; Fig. 4B). The prolonged exposure to the highest concentration of aflibercept (1000 µg/mL) for 48 hours could also intensify the oxidative stress by almost 1.3-fold compared to the control ($P = 0.001$; see Fig. 4B), whereas the shorter incubation with aflibercept for 24 hours failed to induce any effects (see Fig. 4A).

No notable differences in the ROS levels were detected in the Mel270 cells that were treated with ranibizumab or bevacizumab after 24 or 48 hours compared to the controls (see Figs. 4A, 4B). Likewise, the extent of oxidative stress was not altered in the OMM2.5 cells in response to any of the test substances (Figs. 4C, 4D).

Expression of $VEGFA_{165}$ and VEGFR2

In the Mel270 cells, the immunoreactivity for $VEGFA_{165}$ was not significantly altered in response to any of the test substances compared to control after 24 or 48 hours (Figs. 5A, 5B, see Supplementary Fig. S1). Likewise, the OMM2.5 cells that were exposed to the test substances for 24 hours did not exhibit any differences in the intracellular $VEGFA_{165}$ levels with regard to the control (Fig. 5C, see Supplementary Fig. S1). However, the incubation of OMM2.5 cells with the highest dose of aflibercept (1000 µg/mL) for

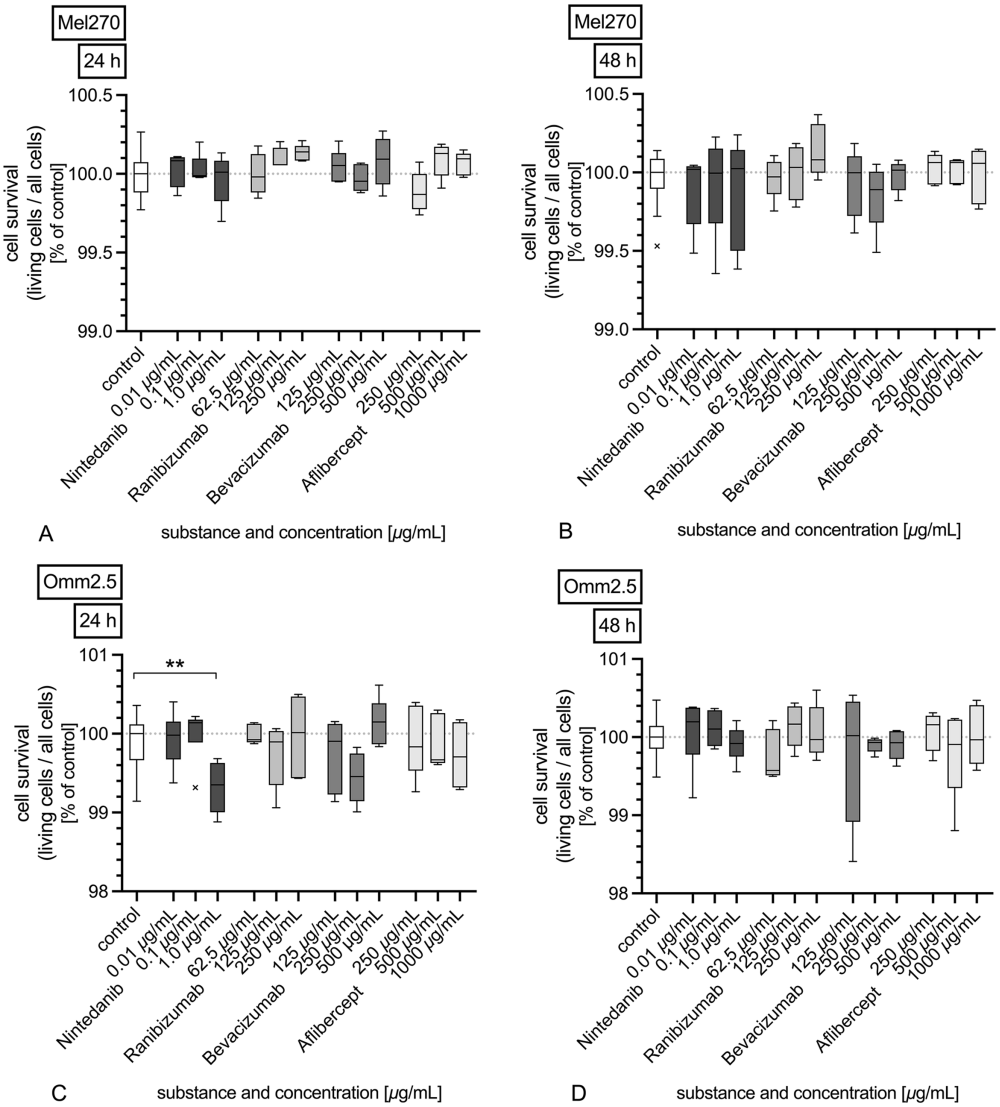

Figure 3. LIVE/DEAD assay demonstrating the cell survival as percentage of untreated control following incubation with nintedanib (0.01; 0.1 and 1 µg/mL), ranibizumab (62.5; 125 and 250 µg/mL), bevacizumab (125; 250 and 500 µg/mL), and aflibercept (250; 500 and 1000 µg/mL) at low, medium, and high concentrations ($n = 3$) for two different incubation durations (24 hours or 48 hours, respectively). The LIVE/DEAD assay aims to discriminate between living cells and dead cells by staining them in different fluorescent dyes (green or red, respectively). Cell survival was calculated by building a quotient out of the area of living cells (pixel) and the total cell area (pixel) for each image. Afterward, data were normalized to the medians of the untreated control of every repetition (n) and therefore data are presented as percentage of untreated control. For a few tested groups statistically extreme outliers (x) were detected as shown in the figure, that represent values of more than three-fold of the interquartile range in Tukey's box plots. (**A**) After 24 hours of incubation, the cell line Mel270 did not exhibit any evidence for substance- or concentration-dependent changes in cell survival or toxic effects. (**B**) Similarly, after 48 hours of incubation, no evidence for changes in cell survival or toxic effects for the cell line Mel270 was shown. (**C**) In contrast, a 24-hour incubation with the high concentration of nintedanib (1 µg/mL) on the cell line OMM2.5 showed a slight decrease in cell survival in comparison with the untreated control ($P = 0.003$ **, Mann Whitney U test). However, the ordinate axis was expanded to accentuate this finding and all concentration groups had a cell survival of approximately 99%, ruling out any relevant toxic effects. (**D**) After the 48 hours of incubation of the OMM2.5 cells with different test substances, there was no evidence of substance- or concentration-dependent changes in cell survival or toxic effects.

48 hours resulted in a 1.4-fold increase in the $VEGFA_{165}$ expression compared to the control ($P = 0.004$; Fig. 5D), whereas aflibercept at lower doses or the remaining test substances failed to induce any effects on the intracellular $VEGFA_{165}$ in the OMM2.5 cells after 48 hours (see Fig. 5D, Supplementary Fig. S1).

No significant differences were observed in the expression of VEGFR2 in the Mel270 or OMM2.5 cells regardless of the test substance and incubation time (Fig. 6, see Supplementary Fig. S1).

Extracellular $VEGFA_{165}$ Levels in Response to the Test Substances After 24 Hours

By performing ELISA, we were not able to detect any $VEGFA_{165}$ in the supernatants of the Mel270 and OMM2.5 cells that were incubated with the anti-VEGFA agents ranibizumab, bevacizumab, and aflibercept ($n = 2$ experiments, data not shown). In both the Mel270 and OMM2.5 cells, the extracellular $VEGFA_{165}$ levels tended to be slightly reduced in response to the highest concentration of

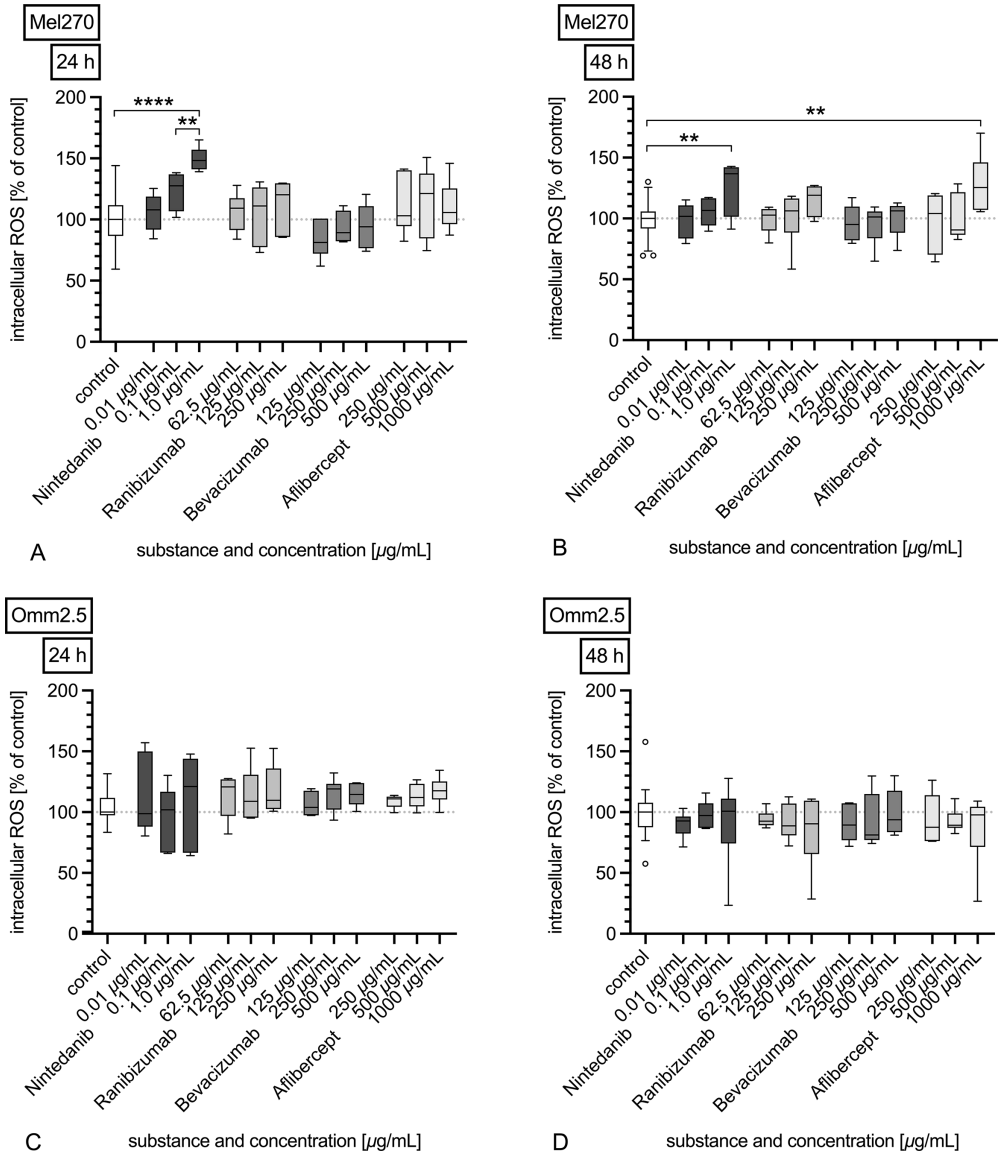

Figure 4. Intracellular reactive oxygen species (ROS) in the cell lines Mel270 and OMM2.5 (as percentage of the untreated control) after 24 or 48 hours of incubation with nintedanib (0.01; 0.1 and 1 µg/mL), ranibizumab (62.5; 125 and 250 µg/mL), bevacizumab (125; 250 and 500 µg/mL), or aflibercept (250; 500 and 1000 µg/mL) at low, medium, and high concentrations ($n = 3$). The amount of intracellular ROS is interpreted as intracellular oxidative stress level of the cells. Values were measured by fluorometry (relative fluorescence units [RFUs]) at the wavelengths of 487 nm and 532 nm. Data were normalized to the medians of the untreated control of every repetition (n) and therefore data are presented as percentage of untreated control. For the control groups statistically simple outliers (degrees) were detected as shown in the figure, that represent values of more than 1.5-fold of the interquartile range in Tukey's box plots. (**A**) Incubation of the Mel270 cells with nintedanib for 24 hours increased the intracellular ROS levels in a dose dependent manner, with the highest oxidative stress detected for 1 µg/mL ($P < 0.001$ **** and $P = 0.002$ **). (**B**) The oxidative stress in response to 1 µg/mL nintedanib was sustained after 48 hours in the Mel270 cells ($P = 0.01$ **). The 48-hour incubation of the Mel270 cells with aflibercept at the highest concentration (1000 µg/mL) also resulted in a higher ROS level than the untreated control ($P = 0.001$ **). For the cell line OMM2.5, no substance or concentration dependent changes in intracellular ROS could be detected neither for (**C**) 24 hours of incubation, nor for (**D**) 48 hours.

nintedanib compared to the intermediate and lower doses of this inhibitor, which did not reach significance (Figs. 7A, 7B).

Discussion

Incubation of the Mel270 and OMM2.5 cells with the multi-angiokinase inhibitor nintedanib at the highest tested concentration (1 µg/mL) resulted in a reduction of metabolic activity without showing explicit toxic effects. In contrast to OMM2.5, the Mel270 cells furthermore presented an elevated oxidative stress under treatment with 1 µg/mL nintedanib. The VEGF-A inhibitors ranibizumab, bevacizumab, and aflibercept were able to fully block the secreted VEGF-A_{165} in the medium supernatants (data not shown), whereas nintedanib failed to exert any effects on the extracellular VEGF-A_{165}. However, ranibizumab, bevacizumab and aflibercept remained mostly inefficient by comparison with controls regarding the metabolic activity and oxidative stress. We were not able to detect any alterations in the cellular expression of VEGF-A_{165}

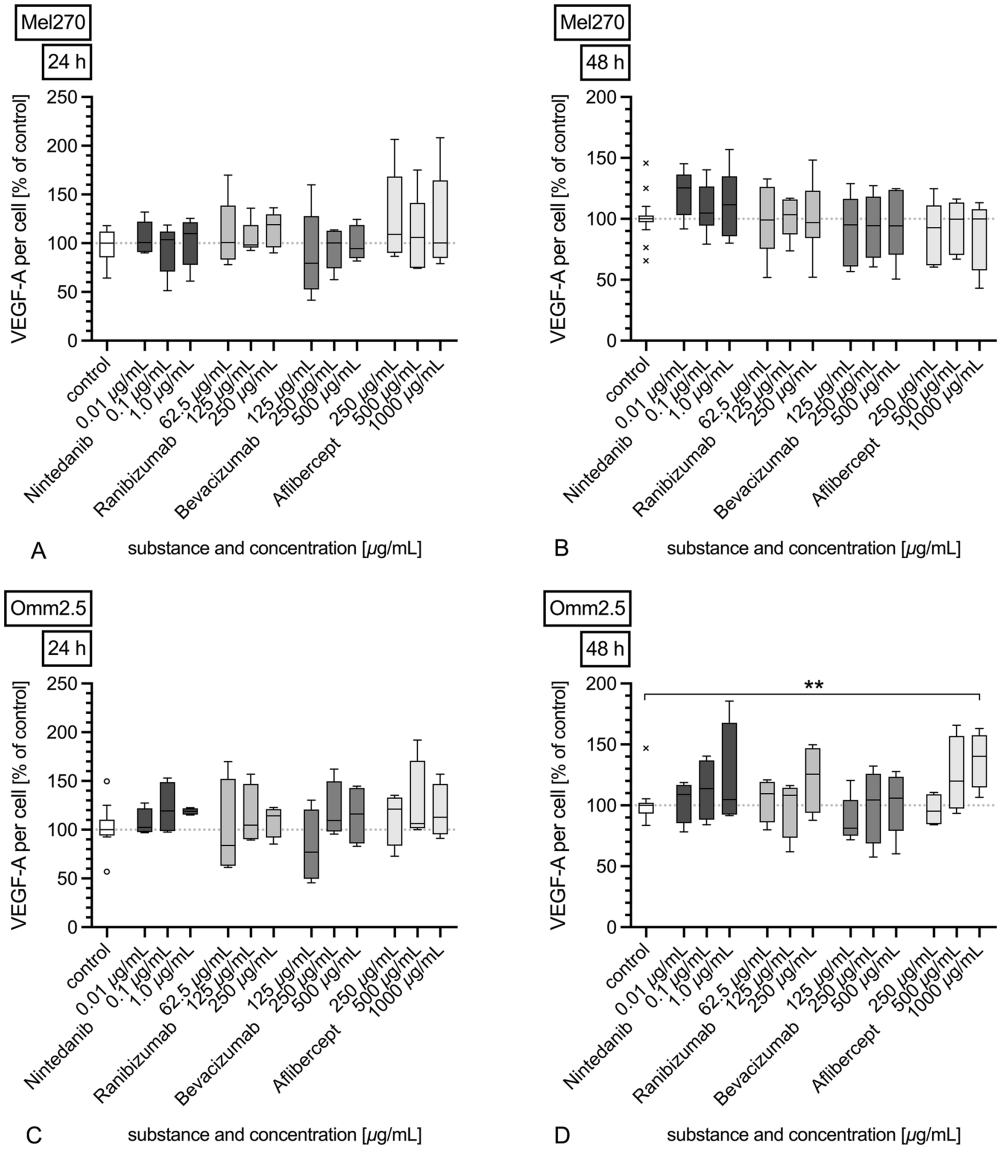

Figure 5. Immunofluorescent staining for intracellular VEGF-A_{165} in the cell lines Mel270 and OMM2.5. The VEGF-A_{165} levels were measured semiquantitatively as fluorescent stained area (VEGF-A_{165}) of each image per mean cell nucleus area (DAPI; in pixels) and expressed as the percentage of the untreated control after 24 (**A** and **C**) or 48 hours (**B** and **D**) of incubation with nintedanib (0.01; 0.1 and 1 µg/mL), ranibizumab (62.5; 125 and 250 µg/mL), bevacizumab (125; 250 and 500 µg/mL), or aflibercept (250; 500 and 1000 µg/mL) at low, medium, and high concentrations. The replicate numbers were $n = 5$ (**A**), $n = 6$ (**B**), $n = 4$ (**C**), and $n = 5$ (**D**), respectively. For the control groups statistically simple (degrees) and extreme outliers (^{x}) were detected as shown in the figure, that represent values of more than 1.5- or 3-fold of the interquartile range in Tukey's box plots. Data were normalized to the medians of the untreated control of every repetition (n) and therefore data are presented as percentage of untreated control. Incubation of the OMM2.5 cells with 1000 µg/mL aflibercept for 48 hours resulted in a higher amount of VEGF-A_{165} in comparison with the control group ($P = 0.004$ **). No changes in intracellular VEGF-A_{165} levels were detected for the remaining treatment groups (**A–D**).

or VEGFR2 in response to any of the test substances either.

The MTT assay is a long established, cost effective, and rapidly applied method as part of the drug discovery processes.[64–66,77] It helps identify potential candidates by evaluating their impact on cell viability and proliferation, especially in the field of sensitivity testing just as in this present study.[78–83] In this study, the MTT assay[64,66,77,79–85] was performed to screen different concentrations of the four substances. Nintedanib, at a concentration of 1 µg/mL, showed an anti-proliferative effect by reducing the metabolic activity of the 2 UM cell lines. Such an effect of this substance has not been reported for UM yet, but similar effects of nintedanib on lung cancer cell lines have been described, in which the dimensions of metabolic reduction have been comparable with our results.[86]

Our findings, that none of the 3 other substances (ranibizumab, bevacizumab, or aflibercept) induced any toxic effects on the two UM cell lines, may initially appear to be contradictory to our earlier study, which demonstrated a significant reduction in the metabolic activity of the Mel270 and OMM2.5 cells that were treated with ranibizumab for 1 day.[87] However, our former MTT analysis was conducted by using a culture medium with 5% serum, whereas, in our

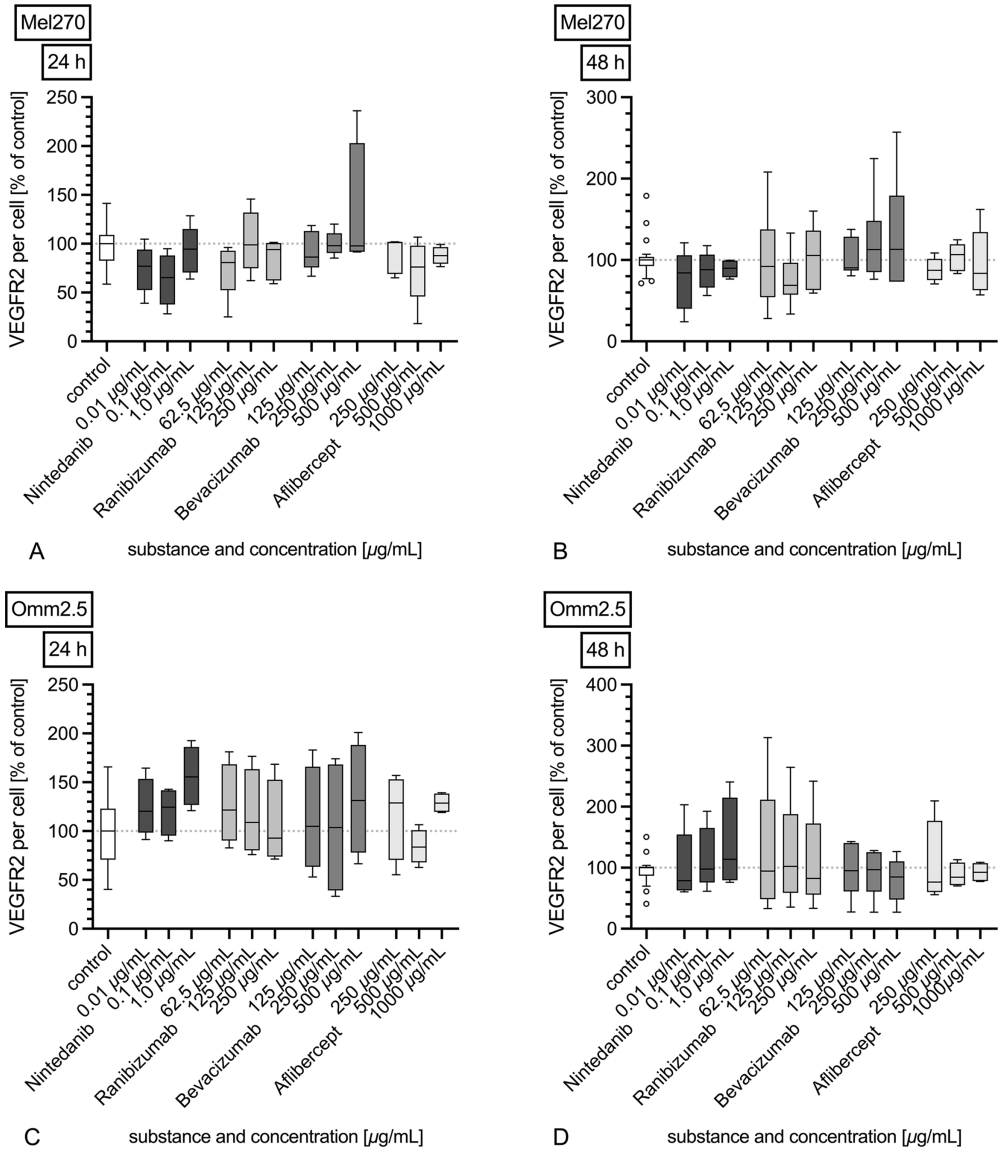

Figure 6. Expression of VEGF receptor-2 (VEGFR2) in the cell lines Mel270 and OMM2.5, as detected by immunofluorescent staining. The VEGFR2 levels were measured semiquantitatively as fluorescent stained area (VEGFR2) of each image per mean cell nucleus area (DAPI; in pixels) and expressed as the percentage of untreated control after 24 hours (**A** and **C**) or 48 hours (**B** and **D**) of incubation with nintedanib (0.01; 0.1 and 1 µg/mL), ranibizumab (62.5; 125 and 250 µg/mL), bevacizumab (125; 250 and 500 µg/mL), or aflibercept (250; 500 and 1000 µg/mL) at low, medium, and high concentrations with replicate numbers of $n = 6$ (**A**), $n = 7$ (**B**), $n = 4$ (**C**), and $n = 5$ (**D**). For the control groups statistically simple outliers (degrees) were detected as shown in the figure, that represent values of more than 1.5-fold of the interquartile range in Tukey's box plots. Data were normalized to the medians of the untreated control of every repetition (n) and therefore data is presented as percentage of untreated control. There was no evidence for substance- or concentration- dependent changes in the expression of VEGFR2 (**A–D**).

present work, the test substances were administered into the complete culture medium with 10% serum for the MTT assay. The higher serum levels in our current study might therefore have increased the abundance of VEGF-A_{165} in the microenvironment, rendering the ranibizumab treatment inefficient for the suppression of metabolic activity. Our new results with ranibizumab, bevacizumab, and aflibercept are also in accordance with earlier findings that could not demonstrate any harm on nonmalignant ocular cells.[88–90] On the other hand, in situ experiments with patients suffering from adenocarcinoma of the intestine showed an enhanced apoptosis of tumor cells under treatment with bevacizumab.[91] Incongruent results were delivered by the research group of Adamcic et al. that tested the proliferation of human melanoma cell lines in response to bevacizumab, where one cell line underwent no change, whereas the other cell line started to proliferate more.[30] The second cell line in that study, however, acquired an anti-proliferative phenotype in response to sunitinib, which is another inhibitor of multiple receptor tyrosine kinases that include the VEGFR2.[30] This shows how receptor inhibition versus substrate inhibition can have opposite effects, and how the actual results may depend on the cell culture entity. In connection with the previously mentioned "paradoxical" growth of UM in the eyes of patients following intravitreal bevacizumab administration, various explanatory approaches have also been

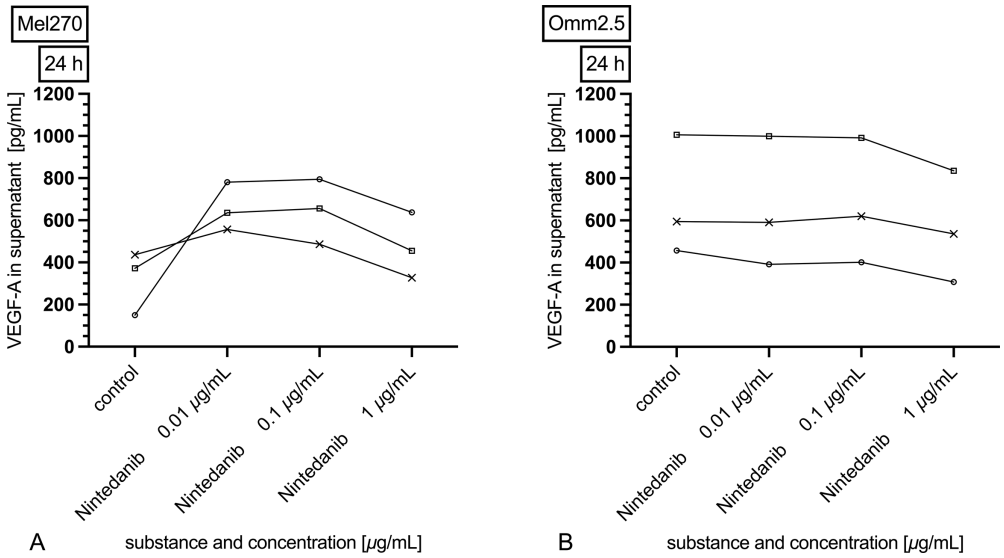

Figure 7. Extracellular VEGF-A_{165} as determined by ELISA. The VEGF-A_{165} concentrations (pg/mL) in the supernatants of the cell lines Mel270 (**A**) and OMM2.5 (**B**) are demonstrated for the untreated controls and cells that were treated with the indicated concentrations of nintedanib (0.01; 0.1 and 1 µg/mL) for 24 hours ($n = 3$ independent experiments that are individually shown [□ × ○]). The data for the three other substances ranibizumab, bevacizumab, and aflibercept are not shown due to the failure of ELISA to detect any VEGF-A_{165} in the supernatants that had been incubated with these substances ($n = 2$), this could be a representation of competitive bindings sites of the ELISA test kit and the test substances themselves binding VEGF-A_{165}.

proposed.[40,41] Different VEGF isoforms may contribute to both angiogenic and anti-angiogenic influences potentially shifting the tumor's milieu toward angiogenic and also proliferative properties by VEGF inhibition.[92] A similar influence can occur through isoforms that either positively or negatively affect cell migratory or proliferative processes.[93] Additionally, activation of vasculogenic mimicry has been suggested as a resistance mechanism to VEGF-A inhibition,[94] as well as a potential rebound effect due to the cessation of such therapy.[40]

Inducing oxidative stress or changing redox balancing is a generally used principle in cancer therapy.[95–100] ROS are chemically reactive molecules that develop during cell metabolism. Although these molecules are often regarded as waste products that the cells have to get rid of to avoid DNA damage, on the other hand, ROS function as signaling molecules as well.[101,102] These cell signaling pathways may have influence on cell survival, inflammation, and tumor progression.[103] Tumor cells often exhibit higher levels of ROS production compared to normal cells due to changes in redox balance.[103] Some anticancer drugs or radiation therapy use generation of ROS as part of their mechanisms of action to utilize the damaging effects of oxidative stress.[95–98,100] In the literature, there are articles that attribute a protective effect to nintedanib against oxidative stress. For instance, Boxhammer et al., 2020, demonstrated in vitro that nintedanib at concentrations of 25 to 100 nM could protect against induction of ROS (via DCFDA assay) by Cyclosporin A in lung fibroblasts. However, the authors acknowledged that the underlying molecular mechanism remains unclear.[104] It is speculated that excessive ROS production may function as a signaling molecule for the release of growth factors. A number of growth factors, particularly PDGF, VEGF, and FGF (the receptors of which are inhibited by nintedanib), can themselves generate ROS, potentially creating a vicious cycle.[105–108] On the other hand, VEGF/VEGFR signaling is involved in the modulation of redox status of cells through multiple signaling pathways. It has been described that VEGF contributes to the reduction of the oxidative environment, thereby protecting cells from oxidative stress, in part by inducing antioxidant enzymes. Disruption of these protective systems through VEGF inhibition can lead to oxidative stress and cell damage.[109–114] The primary tumor cell line Mel270 showed the elevation of ROS in the associated assay[115–119] with the increasing concentrations of nintedanib, which can be interpreted as general oxidative stress[119] induced by this substance. The pro-oxidant effect of nintedanib was shown after 24 hours as well as 48 hours, which corroborates this finding. Elevation of oxidative stress in Mel270 by nintedanib 1 µg/mL may be a sign for a potential anticancer drug effect. On the contrary, OMM2.5 did not show any changes in ROS levels in response to nintedanib. Thus, the metastatic cell line OMM2.5 could be less sensitive to this substance due to the possible adaptations that were acquired during the metastatic evolution. Such adaptation mechanisms for dealing with ROS and oxidative stress have indeed been reported for other cancer cells (like human breast cancer[120]) by boosting the anti-oxidative capacity.[103] On the other hand, cell features could also be changed during cell lines' culture.[57]

Due to the mode of operation of the three anti-VEGF substances ranibizumab, bevacizumab, and aflibercept – and the principle of the VEGF-A_{165} ELISA, it could be shown that these substances were able to effectively block secreted VEGF-A_{165} in the supernatants of both cell lines. However, it remains unclear in this experiment whether VEGF-A_{165} secretion was influenced by these substances or whether the test substances interfered with the ELISA procedure by competing with the assay antibodies to bind VEGF.[121] With ELISA, we observed a slight reduction in VEGF-A_{165} secretion in supernatants of Mel270 and OMM2.5 cells that were incubated with nintedanib at 1 µg/mL. This conclusion should be regarded cautiously due to data spread. Semiquantitative

assessment of both intracellular VEGF-A_{165} and VEGFR2 was not able to show any changes in response to any of the test substances. This may initially appear to contradict with our earlier findings, where we demonstrated a 25% to 45% reduction in intracellular VEGFA in the Mel270 and OMM2.5 cells that were exposed for 1 day to ranibizumab at the concentrations of 125 and 250 µg/mL.[87] However, in our former study, ranibizumab was introduced into a culture medium with 5% serum, whereas our current study was conducted by using a "lighter" medium with 1% serum for the treatment with the test substances. The depletion of some serum-derived factors in our current work may therefore have created a more stringent microenvironment that could have influenced the expression of VEGF-A, which remains to be further investigated. We therefore concluded that we could not provide evidence for a strong direct feedback loop between VEGF-A_{165} or VEGFR2 secretion and VEGF-A_{165} or VEGFR2 inhibition, although the previously discussed experiments were able to show auto- or paracrine influence on cell behavior.[36,37,46,87]

Despite these achieved results, some aspects limit this work. For instance, the LIVE/DEAD assay or the immunostainings for VEGF-A_{165} and VEGFR2 could only be analyzed in a semiquantitative manner, with the threshold for positivity of fluorescence being manually adjusted. However, taking three random pictures per well, blinding the images, and handling them in the same manner minimized intrapersonal deviation and made the analysis as objective as possible. The semiquantitative way of analysis has led to higher variability of results that potentially prohibited finding significant differences between the tested groups. We therefore suggest to explore not only possible alterations of VEGF-A_{165} and VEGFR2 but also other relevant signaling pathways relevant for nintedanib like PDGF or FGF and its receptors through other experimental settings like the more quantitative approach of Western blot, flow cytometry[122] or real time PCR.[123] For an even more precise analysis of the effects of the test substances on oxidative stress, it would have been advisable to include a baseline measurement of ROS in the experiments. This should be taken into consideration in the future. Our experiments were also restricted to only two UM cell lines, which limits possible conclusions for in vivo systems and even for cell culture experiments with other cell lines. Nevertheless, our work may offer interesting starting points for further research such as co-culturing or in vivo models. We would first suggest including additional UM cell lines. It may be beneficial to consider different characteristics of tumor aggressiveness in these cell lines, such as the very important monosomy 3 status[124,125] or others like mitotic rate and the capacity for vasculogenic mimicry.[126] Additionally, we recommend broadening the study approaches by conducting co-culture experiments with other cell types, like endothelial cells, fibroblasts,[127,128] or tumor lymphocytes.[129–131] This would shift the focus to the possibilities of influencing the tumor microenvironment. Particularly for nintedanib, further exploration of possible antitumoral effects through modulation of the tumor microenvironment appears intriguing and should be investigated more closely for its potential in the context of UM. For instance, favorable effects of nintedanib's anti-fibrotic action have already been demonstrated in vitro for other melanoma cells as well as in a melanoma mouse model.[132,133] Furthermore, inhibition of vasculogenic mimicry has been observed in cell culture experiments involving vemurafenib-resistant melanoma cells.[134] It may be of interest to investigate whether the inhibition of TGF-β by nintedanib could lead to alterations in the preference of UM for the liver as its primary metastatic organ. This is prompted by findings indicating that TGF-β could enhance the adhesion of noninvasive UM cells to hepatic endothelium.[135] Certainly, such in vitro approaches cannot be directly extrapolated to in vivo models. However, if promising results continue to emerge, our next recommended step would involve evaluating the exploration of nintedanib in an animal model. Nintedanib has already been clinically approved for human use. Nevertheless, there is currently no available knowledge regarding the use of nintedanib in patients with UM. Whether the substance's mechanism of action could be effective and safe in human UM cannot be asserted at this time. The indispensable final step would involve investigating the effects of the substance in clinical research to gain insights.

Inhibiting tumor angiogenesis is an interesting approach for at least adjuvant tumor therapy,[35,136] however, for UM, there has not yet been a breakthrough in this field of research.[20,137] In clinical studies, angiogenesis inhibitors have only shown a tendency to stabilize the disease, but they have not provided a change in overall survival.[138–143] Generally, the concept of anti-angiogenesis has its limitations also due to resistance mechanisms of tumors and the tumor microenvironment, which may bypass possible therapy effects.[103,128,144–154] This study provides evidence that, unlike the VEGF-A_{165} specific inhibition by ranibizumab, bevacizumab, and aflibercept, a more wide-ranging mechanism of action, provided by the multi-angiokinase inhibitor nintedanib, has an influence on UM cell behaviour, at least in our in vitro experiments. Discovering multiple different treatment options for UM is an important strategy in this field of research and novel anti-angiogenic drugs should among other mechanisms of action remain in the spotlight to gain knowledge. This could lead to different treatment options in consideration of personalized or precision medicine.[155] There could be patients whose tumors may possibly be more sensitive to influence of pro-angiogenic factors. Therefore, by understanding the molecular underpinnings of a patient's cancer, clinicians could select drugs like nintedanib as appropriate treatment options at least in combination with drugs of other target mechanisms. This could minimize the use of the one-size-fits-all approaches and reduce the risk of ineffective treatments.[155]

We suggest further investigation of the mechanisms and effects of signaling pathways for nintedanib in UM. In addition, in vivo models should be established for this purpose in the future.

Acknowledgments

Funded through third-party funding awarded to Mahdy Ranjbar as part of a funding project by the NOVARTIS PHARMA GERMANY. The funders had no influence on the study design, data collection, data processing, the interpretation of the data, or the writing of this paper.

Disclosure: **V.E. Pawlik**, None; **S.R. Sonntag**, None; **S. Grisanti**, None; **A. Tura**, Novartis Pharma Germany (F); **V. Kakkassery**, None; **M. Ranjbar**, Novartis Pharma Germany (F)

References

1. Shields CL, Kaliki S, Furuta M, Mashayekhi A, Shields JA. Clinical spectrum and prognosis of uveal melanoma

based on age at presentation in 8,033 cases. *Retina.* 2012;32(7):1363–1372.
2. Virgili G, Gatta G, Ciccolallo L, et al. Incidence of uveal melanoma in Europe. *Ophthalmology.* 2007;114(12):2309–2315.
3. Singh AD, Turell ME, Topham AK. Uveal melanoma: trends in incidence, treatment, and survival. *Ophthalmology.* 2011;118(9):1881–1885.
4. Singh A, Bergman L, Seregard S. Uveal melanoma: epidemiologic aspects. *Ophthalmol Clin North Am.* 2005;18(1):75–84.
5. Muller K, Nowak PJCM, de Pan C, et al. Effectiveness of fractionated stereotactic radiotherapy for uveal melanoma. *Int J Radiat Oncol Biol Phys.* 2005;63(1):116–122.
6. Simpson ER, Gallie B, Laperrierre N, et al. The American Brachytherapy Society consensus guidelines for plaque brachytherapy of uveal melanoma and retinoblastoma. *Brachytherapy.* 2014;13(1):1–14.
7. Brewington BY, Shao YF, Davidorf FH, Cebulla CM. Brachytherapy for patients with uveal melanoma: historical perspectives and future treatment directions. *Clin Ophthalmol.* 2018;12:925–934.
8. Gündüz K, Bechrakis N. Exoresection and endoresection for uveal melanoma. *Middle East Afr J Ophthalmol.* 2010;17(3):210–216.
9. Collaborative Ocular Melanoma Study Group. The Collaborative Ocular Melanoma Study (COMS) randomized trial of pre-enucleation radiation of large choroidal melanoma III: local complications and observations following enucleation COMS report no. 11. *Am J Ophthalmol.* 1998;126(3):362–372.
10. Kersten RC, Tse DT, Anderson RL, Blodi FC. The role of orbital exenteration in choroidal melanoma with extrascleral extension. *Ophthalmology.* 1985;92(3):436–443.
11. Isager P, Ehlers N, Urbak SF, Overgaard J. Visual outcome, local tumour control, and eye preservation after ^{106}Ru/Rh brachytherapy for choroidal melanoma. *Acta Oncol.* 2006;45(3):285–293.
12. Krantz BA, Dave N, Komatsubara KM, Marr BP, Carvajal RD. Uveal melanoma: epidemiology, etiology, and treatment of primary disease. *Clin Ophthalmol.* 2017;11:279–289.
13. Diener-West M, Reynolds SM, Agugliaro DJ, et al. Development of metastatic disease after enrollment in the COMS trials for treatment of choroidal melanoma: collaborative ocular melanoma study group report no. 26. *Arch Ophthalmol.* 2005;123(12):1639–1643.
14. Bakalian S, Marshall JC, Logan P, et al. Molecular pathways mediating liver metastasis in patients with uveal melanoma. *Clin Cancer Res.* 2008;14(4):951–956.
15. Jager MJ, Shields CL, Cebulla CM, et al. Uveal melanoma. *Nat Rev Dis Primers.* 2020;6(1):24.
16. Krishna Y, McCarthy C, Kalirai H, Coupland SE. Inflammatory cell infiltrates in advanced metastatic uveal melanoma. *Human Pathol.* 2017;66:159–166.
17. Howlett S, Carter TJ, Shaw HM, Nathan PD. Tebentafusp: a first-in-class treatment f or metastatic uveal melanoma. *Ther Adv Med Oncol.* 2023;15: 175883592311601.
18. Ferrara N. VEGF and the quest for tumour angiogenesis factors. *Nat Rev Cancer.* 2002;2(10):795–803.
19. Folkman J. Anti-angiogenesis: new concept for therapy of solid tumors. *Ann Surg.* 1972;175(3):409–416.
20. Castet F, Garcia-Mulero S, Sanz-Pamplona R, et al. Uveal melanoma, angiogenesis and immunotherapy, is there any hope? *Cancers (Basel).* 2019;11(6):834.
21. Boocock CA, Charnock-Jones DS, Sharkey AM, et al. Expression of vascular endothelial growth factor and its receptors flt and KDR in ovarian carcinoma. *J Natl Cancer Inst.* 1995;87(7):506–516.
22. Masood R, Cai J, Zheng T, Smith DL, Hinton DR, Gill PS. Vascular endothelial growth factor (VEGF) is an autocrine growth factor for VEGF receptor–positive human tumors. *Blood.* 2001;98(6):1904–1913.
23. Neuchrist C, Erovic BM, Handisurya A, et al. Vascular endothelial growth factor receptor 2 (VEGFR2) expression in squamous cell carcinomas of the head and neck. *Laryngoscope.* 2001;111(10):1834–1841.
24. Gee MFW, Tsuchida R, Eichler-Jonsson C, Das B, Baruchel S, Malkin D. Vascular endothelial growth factor acts in an autocrine manner in rhabdomyosarcoma cell lines and can be inhibited with all-trans-retinoic acid. *Oncogene.* 2005;24(54):8025–8037.
25. Xia G, Kumar SR, Hawes D, et al. Expression and significance of vascular endothelial growth factor receptor 2 in bladder cancer. *J Urol.* 2006;175(4):1245–1252.
26. Lee TH, Seng S, Sekine M, et al. Vascular endothelial growth factor mediates intracrine survival in human breast carcinoma cells through internally expressed VEGFR1/FLT1. Kerbel RS, Herausgeber. *PLoS Med.* 2007;4(6):e186.
27. Aesoy R, Sanchez BC, Norum JH, Lewensohn R, Viktorsson K, Linderholm B. An autocrine VEGF/VEGFR2 and p38 signaling loop confers resistance to 4- hydroxytamoxifen in MCF-7 breast cancer cells. *Mol Cancer Res.* 2008;6(10):1630–1638.
28. Nakanishi R, Oka N, Nakatsuji H, et al. Effect of vascular endothelial growth factor and its receptor inhibitor on proliferation and invasion in bladder cancer. *Urol Int.* 2009;83:98–106.
29. Takahashi S. Vascular endothelial growth factor (VEGF), VEGF receptors and their inhibitors for antiangiogenic tumor therapy. *Biol Pharm Bull.* 2011;34(12):1785–1788.
30. Adamcic U, Skowronski K, Peters C, Morrison J, Coomber BL. The effect of bevacizumab on human malignant melanoma cells with functional VEGF/VEGFR2 autocrine and intracrine signaling loops. *Neoplasia.* 2012;14(7):612–623.
31. Chatterjee S, Heukamp LC, Siobal M, et al. Tumor VEGF:VEGFR2 autocrine feed- forward loop triggers angiogenesis in lung cancer. *J Clin Invest.* 2013;123(4):1732–1740.
32. Bhattacharya R, Fan F, Wang R, et al. Intracrine VEGF signalling mediates colorectal cancer cell migration and invasion. *Br J Cancer.* 2017;117(6):848–855.
33. el Filali M, Van der Velden PA, Luyten GPM, Jager MJ. Anti-angiogenic therapy in uveal melanoma. In: Jager MJ, Desjardins L, Kivelä T, Damato B, eds. *Developments in Ophthalmology.* Basel, Switzerland: KARGER. 2011;S117–S136.
34. Croce M, Ferrini S, Pfeffer U, Gangemi R. Targeted therapy of uveal melanoma: recent failures and new perspectives. *Cancers (Basel).* 2019;11(6):846.
35. Lugano R, Ramachandran M, Dimberg A. Tumor angiogenesis: causes, consequences, challenges and opportunities. *Cell Mol Life Sci.* 2020;77(9):1745–1770.
36. Stitt AW, Simpson DAC, Boocock C, Gardiner TA, Murphy GM, Archer DB. Expression of vascular endothelial growth factor (VEGF) and its receptors is regulated in eyes with intra-ocular tumours. *J Pathol.* 1998;186(3):306–312.
37. el Filali M, Missotten GSOA, Maat W, et al. Regulation of VEGF-A in uveal melanoma. *Invest Ophthalmol Vis Sci.* 2010;51(5):2329–2337.
38. Yang H, Jager MJ, Grossniklaus HE. Bevacizumab suppression of establishment of micrometastases in experimental ocular melanoma. *Invest Ophthalmol Vis Sci.* 2010;51(6):2835–2842.

39. el Filali M, Ly LV, Luyten GPM, et al. Bevacizumab and intraocular tumors: an intriguing paradox. *Mol Vis.* 2012;18:2454–2467.
40. Ma J, Roelofs KA, Russell L, Weis E, Chen SH. Rapid growth of primary uveal melanoma following intravitreal bevacizumab injection: a case report and review of the literature. *Digit J Ophthalmol. 3.* 2020;26(3):27–30.
41. Francis JH, Kim J, Lin A, Folberg R, Iyer S, Abramson DH. Growth of uveal melanoma following intravitreal bevacizumab. *Ocul Oncol Pathol.* 2017;3(2):117–121.
42. Stacey AW, Demirci H. Serial intravitreal bevacizumab injections slow the progression of radiation maculopathy following iodine-125 plaque radiotherapy. *Open Ophthalmol J.* 2016;10(1):103–110.
43. Ijland S, Jager MJ, Heijdra B, Westphal J, Peek R. Expression of angiogenic and immunosuppressive factors by uveal melanoma cell lines. *Melanoma Res.* 1999;9(5):445–450.
44. Notting IC, Missotten GSOA, Sijmons B, Boonman ZFHM, Keunen JEE, van der Pluijm G. Angiogenic profile of uveal melanoma. *Curr Eye Res.* 2006;31(9):775–785.
45. Franco R, Botti G, Mascolo M, et al. CXCR4-CXCL12 and VEGF correlate to uveal melanoma progression. *Front Biosci (Elite Ed).* 2010;2(1):13–21.
46. Koch KR, Refaian N, Hos D, et al. Autocrine impact of VEGF-A on uveal melanoma cells. *Invest Ophthalmol Vis Sci.* 2014;55(4):2697–7204.
47. Eide N, Hoifødt HK, Nesland JM, et al. Disseminated tumour cells in bone marrow of patients with uveal melanoma. *Acta Ophthalmol.* 2013;91(4):343–348.
48. Ferrara N, Damico L, Shams N, Lowman H, Kim R. Development of ranibizumab, an anti-vascular endothelial growth factor antigen binding fragment, as therapy for neovascular age-related macular degeneration. *Retina.* 2006;26(8):859–870.
49. Ferrara N, Hillan KJ, Gerber HP, Novotny W. Discovery and development of bevacizumab, an anti-VEGF antibody for treating cancer. *Nat Rev Drug Discov.* 2004;3(5):391–400.
50. Holash J, Davis S, Papadopoulos N, et al. VEGF-Trap: a VEGF blocker with potent antitumor effects. *Proc Natl Acad Sci USA.* 2002;99(17):11393–11398.
51. Hilberg F, Roth GJ, Krssak M, et al. BIBF 1120: triple angiokinase inhibitor with sustained receptor blockade and good antitumor efficacy. *Cancer Res.* 2008;68(12):4774–4782.
52. Roth GJ, Heckel A, Colbatzky F, et al. Design, synthesis, and evaluation of indolinones as triple angiokinase inhibitors and the discovery of a highly specific 6- methoxycarbonyl-substituted indolinone (BIBF 1120). *J Med Chem.* 2009;52(14):4466–4480.
53. Reck M. Nintedanib: examining the development and mechanism of action of a novel triple angiokinase inhibitor. *Expert Rev Anticancer Ther.* 2015;15(5):579–594.
54. Chen PW, Murray TG, Uno T, Salgaller ML, Reddy R, Ksander BR. Expression of MAGE genes in ocular melanoma during progression from primary to metastatic disease. *Clin Exp Metastasis.* 1996;15(5):509–518.
55. Verbik DJ, Murray TG, Tran JM, Ksander BR. Melanomas that develop within the eye inhibit lymphocyte proliferation. *Int J Cancer.* 1997;73(4):470–478.
56. Gupta GP, Massagué J. Cancer metastasis: building a framework. *Cell.* 2006;127(4):679–695.
57. Jager MJ, Magner JAB, Ksander BR, Dubovy SR. Uveal melanoma cell lines: where do they come from? (An American Ophthalmological Society Thesis). *Trans Am Ophthalmol Soc.* 2016;114:T5(1-16).
58. Angi M, Versluis M, Kalirai H. Culturing uveal melanoma cells. *Ocul Oncol Pathol.* 2015;1(3):126–132.
59. Lundberg AS, Weinberg RA. Control of the cell cycle and apoptosis. *Eur J Cancer.* 1999;35(14):1886–1894.
60. European Medicines Agency. Ranibizumab - Anhang I Zusammenfassung der Merkmale des Arzneimittels. Available at: https://www.ema.europa.eu/en/documents/product-information/lucentis-epar-product-information_de.pdf. Accessed June 8, 2023.
61. European Medicines Agency. Bevacizumab - Anhang I Zusammenfassung der Merkmale des Arzneimittels. Available at: https://www.ema.europa.eu/en/documents/product-information/avastin-epar-product-information_de.pdf. Accessed June 8, 2023.
62. Zhao C, Lan B, Hou J, Cheng L. Cytotoxicity of dimethyl sulphoxide on ocular cells in vitro. *Chin J Ophthalmol.* 2015;33(3):216–220.
63. Jamalzadeh L, Ghafoori H, Sariri R, et al. Cytotoxic effects of some common organic solvents on MCF-7, RAW-264.7 and human umbilical vein endothelial cells. *Avicenna J Med Biochem.* 2016;4(1):e33453.
64. Mosmann T. Rapid colorimetric assay for cellular growth and survival: application to proliferation and cytotoxicity assays. *J Immunol Methods.* 1983;65(1–2):55–63.
65. Denizot F, Lang R. Rapid colorimetric assay for cell growth and survival. Modifications to the tetrazolium dye procedure giving improved sensitivity and reliability. *J Immunol Methods.* 1986;89(2):271–277.
66. Twentyman PR, Luscombe M. A study of some variables in a tetrazolium dye (MTT) based assay for cell growth and chemosensitivity. *Br J Cancer.* 1987;56(3):279–285.
67. ThermoFisher Scientific, Molecular Probes invitrogen detection technologies. Reactive Oxygen Species (ROS) Detection Reagents - Pub. No. MAN0002456; Doc. Part. No. MP36103. Available at: https://assets.thermofisher.com/TFS-Assets/LSG/manuals/mp36103.pdf, Revised on January 10, 2006. Accessed June 8, 2023.
68. invitrogen, ThermoFisher Scientific. Live/Dead Cell Imaging Kit No. R37601 Pub. Nr. MAN0006090 Rev. A.0. Available at: https://assets.thermofisher.com/TFS-Assets/LSG/manuals/MAN0006090_LIVE_DEAD_Cell_Imaging_Kit_QR.pdf 2016. Accessed June 8, 2023.
69. Weston SA, Parish CR. New fluorescent dyes for lymphocyte migration studies. Analysis by flow cytometry and fluorescence microscopy. *J Immunol Methods.* 1990;133(1):87–97.
70. De Clerck LS, Bridts CH, Mertens AM, Moens MM, Stevens WJ. Use of fluorescent dyes in the determination of adherence of human leucocytes to endothelial cells and the effect of fluorochromes on cellular function. *J Immunol Methods.* 1994;172(1):115–124.
71. Orchel A, Chodurek E, Jaworska-Kik M, et al. Anticancer activity of the acetylenic derivative of betulin phosphate involves induction of necrotic-like death in breast cancer cells in vitro. *Molecules.* 2021;26(3):615.
72. Schneider CA, Rasband WS, Eliceiri KW. NIH Image to ImageJ: 25 years of image analysis. *Nat Methods.* 2012;9(7):671–675.
73. ThermoFisher Scientific. Human VEGFA ELISA Kit Instructions EH2VEGF EH2VEGF2 EH2VEGF5. Available at: https://assets.fishersci.com/TFS-Assets/LSG/manuals/MAN0011806_Human_VEGFA_ELISA_UG.pdf. Accessed June 8, 2023.
74. Comparison of Age-related Macular Degeneration Treatments Trials (CATT) Research Group; Martin DF, Maguire MG, Ying G, Grunwald JE, Fine SL. Ranibizumab and bevacizumab for neovascular age-related macular degeneration. *N Engl J Med.* 2011;364(20):1897–1908.
75. Malik D, Tarek M, Caceres del Carpio J, et al. Safety profiles of anti-VEGF drugs: bevacizumab, ranibizumab, aflibercept

and ziv-aflibercept on human retinal pigment epithelium cells in culture. *Br J Ophthalmol.* 2014;98(Suppl 1):i11–i16.
76. Lin T, Gong L. Inhibition of lymphangiogenesis in vitro and in vivo by the multikinase inhibitor nintedanib. *Drug Des Devel Ther.* 2017;11:1147–1158.
77. Gerlier D, Thomasset N. Use of MTT colorimetric assay to measure cell activation. *J Immunol Methods.* 1986;94(1–2):57–63.
78. Carmichael J, Mitchell JB, DeGraff WG, et al. Chemosensitivity testing of human lung cancer cell lines using the MTT assay. *Br J Cancer.* 1985;57(6):540–547.
79. Cole SP. Rapid chemosensitivity testing of human lung tumor cells using the MTT assay. *Cancer Chemother Pharmacol.* 1986;17(3):259–263.
80. Finlay GJ, Wilson WR, Baguley BC. Comparison of in vitro activity of cytotoxic drugs towards human carcinoma and leukaemia cell lines. *Eur J Cancer Clin Oncol.* 1986;22(6):655–662.
81. Park JG, Kramer BS, Steinberg SM, et al. Chemosensitivity testing of human colorectal carcinoma cell lines using a tetrazolium-based colorimetrie assay. *Cancer Res.* 1987;47(22):5875–5879.
82. Alley MC, Scudiere DA, Monks A, et al. Feasibility of drug screening with panels of human tumor cell lines using a microculture tetrazolium assay. *Cancer Res.* 1988;48(3):589–601.
83. Ford CH, Richardson VJ, Tsaltas G. Comparison of tetrazolium colorimetric and [3H]- uridine assays for in vitro chemosensitivity testing. *Cancer Chemother Pharmacol.* 1989;24(5):295–301.
84. Green LM, Reade JL, Ware CF. Rapid colorimetric assay for cell viability: application to the quantitation of cytotoxic and growth inhibitory lymphokines. *J Immunol Methods.* 1984;70(2):257–268.
85. Campling BG, Pym J, Baker HM, Cole SP, Lam YM. Chemosensitivity testing of small cell lung cancer using the MTT assay. *Br J Cancer.* 1991;63(1):75–83.
86. Englinger B, Kallus S, Senkiv J, et al. Intrinsic fluorescence of the clinically approved multikinase inhibitor nintedanib reveals lysosomal sequestration as resistance mechanism in FGFR-driven lung cancer. *J Exp Clin Cancer Res.* 2017;36(1):122.
87. Tura A, Pawlik VE, Rudolf M, et al. Uptake of ranibizumab but not bevacizumab into uveal melanoma cells correlates with a sustained decline in VEGF-A levels and metastatic activities. *Cancers.* 2019;11(6):868.
88. Luthra S, Narayanan R, Marques LEA, et al. Evaluation of in vitro effects of bevacizumab (avastin) on retinal pigment epithelial, neurosensory retinal, and microvascular endothelial cells. *Retina.* 2006;26(5):512–518.
89. Brar VS, Sharma RK, Murthy RK, Chalam KV. Evaluation of differential toxicity of varying doses of bevacizumab on retinal ganglion cells, retinal pigment epithelial cells, and vascular endothelial growth factor–enriched choroidal endothelial cells. *J Oncul Pharmacol Ther.* 2009;25(6):507–512.
90. Schnichels S, Hagemann U, Januschowski K, et al. Comparative toxicity and proliferation testing of aflibercept, bevacizumab and ranibizumab on different ocular cells. *Br J Ophthalmol.* 2013;97(7):917–923.
91. Willett CG, Boucher Y, Duda DG, et al. Surrogate markers for antiangiogenic therapy and dose-limiting toxicities for bevacizumab with radiation and chemotherapy: continued experience of a phase I trial in rectal cancer patients. *J Clin Oncol.* 2005;23(31):8136–8139.
92. Kawamura H, Li X, Harper SJ, Bates DO, Claesson-Welsh L. Vascular endothelial growth factor (VEGF)-A165b is a weak in vitro agonist for VEGF receptor-2 due to lack of coreceptor binding and deficient regulation of kinase activity. *Cancer Res.* 2008;68(12):4683–4692.
93. Rennel ES, Waine E, Guan H, et al. The endogenous anti-angiogenic VEGF isoform, VEGF165b inhibits human tumour growth in mice. *Br J Cancer.* 2008;98(7):1250–1257.
94. Schnegg CI, Yang MH, Ghosh SK, Hsu MY. Induction of vasculogenic mimicry overrides VEGF-A silencing and enriches stem-like cancer cells in melanoma. *Cancer Res.* 2015;75(8):1682–1690.
95. Kapitza S, Jakupec MA, Uhl M, Keppler BK, Marian B. The heterocyclic ruthenium(III) complex KP1019 (FFC14A) causes DNA damage and oxidative stress in colorectal tumor cells. *Cancer Lett.* 2005;226(2):115–121.
96. Trachootham D, Alexandre J, Huang P. Targeting cancer cells by ROS-mediated mechanisms: a radical therapeutic approach? *Nat Rev Drug Discov.* 2009;8(7):579–591.
97. Yoshida T, Goto S, Kawakatsu M, Urata Y, Li TS. Mitochondrial dysfunction, a probable cause of persistent oxidative stress after exposure to ionizing radiation. *Free Radic Res.* 2012;46(2):147–153.
98. Gorrini C, Harris IS, Mak TW. Modulation of oxidative stress as an anticancer strategy. *Nat Rev Drug Discov.* 2013;12(12):931–947.
99. Sullivan LB, Chandel NS. Mitochondrial reactive oxygen species and cancer. *Cancer Metab.* 2014;2:17.
100. Yang H, Villani RM, Wang H, et al. The role of cellular reactive oxygen species in cancer chemotherapy. *J Exp Clin Cancer Res.* 2018;37(1):266.
101. Ott M, Gogvadze V, Orrenius S, Zhivotovsky B. Mitochondria, oxidative stress and cell death. *Apoptosis.* 2007;12(5):913–922.
102. Finkel T. Oxygen radicals and signaling. *Curr Opin Cell Biol.* 1998;10(2):248–253.
103. Saikolappan S, Kumar B, Shishodia G, Koul S, Koul HK. Reactive oxygen species and cancer: a complex interaction. *Cancer Lett.* 2019;452:132–143.
104. Boxhammer E, Lehle K, Schmid C, von Suesskind-Schwendi M. Anti-oxidative effect of the tyrosine kinase inhibitor nintedanib: a potential therapy for chronic lung allograft dysfunction? *Exp Lung Res.* 2020;46(5):128–145.
105. Black SM, DeVol JM, Wedgwood S. Regulation of fibroblast growth factor-2 expression in pulmonary arterial smooth muscle cells involves increased reactive oxygen species generation. *Am J Physiol Cell Physiol.* 2008;294(1):C345–C354.
106. Krstić J, Trivanović D, Mojsilović S, Santibanez JF. Transforming growth factor-beta and oxidative stress interplay: implications in tumorigenesis and cancer progression. *Oxid Med Cellul Longev.* 2015;2015:1–15.
107. Thannickal VJ, Fanburg BL. Reactive oxygen species in cell signaling. *Am J Physiol Lung Cell Mol Physiol.* 2000;279(6):L1005–L1028.
108. Sauer H, Wartenberg M, Hescheler J. Reactive oxygen species as intracellular messengers during cell growth and differentiation. *Cell Physiol Biochem.* 2001;11(4):173–186.
109. Chan E, Liu GS, Dusting G. Redox mechanisms in pathological angiogenesis in the retina: roles for NADPH oxidase. *Curr Pharm Des.* 2015;21(41):5988–5998.
110. El-Remessy AB, Bartoli M, Platt DH, Fulton D, Caldwell RB. Oxidative stress inactivates VEGF survival signaling in retinal endothelial cells via PI 3-kinase tyrosine nitration. *J Cell Sci.* 2016;129(16):3203.
111. Schulz E, Jansen T, Wenzel P, Daiber A, Münzel T. Nitric oxide, tetrahydrobiopterin, oxidative stress, and endothelial dysfunction in hypertension. *Antioxid Redox Signal.* 2008;10(6):1115–1126.

112. Yang KS, Lim JH, Kim TW, et al. Vascular endothelial growth factor-receptor 1 inhibition aggravates diabetic nephropathy through eNOS signaling pathway in db/db mice. *PLoS One.* 2014;9(4):e94540.
113. Sheu S, Chao Y, Liu N, Chan JYH. Differential effects of bevacizumab, ranibizumab and aflibercept on cell viability, phagocytosis and mitochondrial bioenergetics of retinal pigment epithelial cell. *Acta Ophthalmologica.* 2015;93(8):e631–e643
114. Matsuda M, Krempel PG, Marquezini MV, et al. Cellular stress response in human Müller cells (MIO-M1) after bevacizumab treatment. *Exp Eye Res.* 2017;160:1–10.
115. LeBel CP, Ali SF, McKee M, Bondy SC. Organometal-induced increases in oxygen reactive species: the potential of 2′,7′-dichlorofluorescin diacetate as an index of neurotoxic damage. *Toxicol Appl Pharmacol.* 1990;104(1):17–24.
116. Mattia CJ, LeBel CP, Bondy SC. Effects of toluene and its metabolites on cerebral reactive oxygen species generation. *Biochem Pharmacol.* 1991;42(4):879–882.
117. LeBel CP, Ali SF, Bondy SC. Deferoxamine inhibits methyl mercury-induced increases in reactive oxygen species formation in rat brain. *Toxicol Appl Pharmacol.* 1992;112(1):161–165.
118. LeBel CP, Ischiropoulos H, Bondy SC. Evaluation of the probe 2',7'-dichlorofluorescin as an indicator of reactive oxygen species formation and oxidative stress. *Chem Res Toxicol.* 1992;5(2):227–231.
119. Jakubowski W, Bartosz G. 2,7-dichlorofluorescin oxidation and reactive oxygen species: what does it measure? *Cell Biol Int.* 2000;24(10):757–760.
120. Diehn M, Cho RW, Lobo NA, et al. Association of reactive oxygen species levels and radioresistance in cancer stem cells. *Nature.* 2009;458(7239):780–783.
121. Takahashi H, Nomura Y, Nishida J, Fujino Y, Yanagi Y, Kawashima H. Vascular endothelial growth factor (VEGF) concentration is underestimated by enzyme-linked immunosorbent assay in the presence of anti-VEGF drugs. *Invest Ophthalmol Vis Sci.* 2016;57(2):462–466.
122. Imoukhuede PI, Popel AS. Quantification and cell-to-cell variation of vascular endothelial growth factor receptors. *Exp Cell Res.* 2011;317(7):955–965.
123. Bonino F, Milanini J, Pouysségur J, Pagès G. RT-PCR method to quantify vascular endothelial growth factor expression. *BioTechniques.* 2001;30(6):1254–1260.
124. Onken MD, Worley LA, Ehlers JP, Harbour JW. Gene expression profiling in uveal melanoma reveals two molecular classes and predicts metastatic death. *Cancer Res.* 2004;64(20):7205–7209.
125. Robertson AG, Shih J, Yau C, et al. Integrative analysis identifies four molecular and clinical subsets in uveal melanoma. *Cancer Cell.* 2017;32(2):204–220.e15.
126. Sahin A, Kiratli H, Soylemezoglu F, Tezel GG, Bilgic S, Saracbasi O. Expression of vascular endothelial growth factor-a, matrix metalloproteinase-9, and extravascular matrix patterns and their correlations with clinicopathologic parameters in posterior uveal melanomas. *Jpn J Ophthalmol.* 2007;51(5):325–331.
127. Orimo A, Weinberg RA. Stromal fibroblasts in cancer: a novel tumor-promoting cell type. *Cell Cycle.* 2006;5(15):1597–1601.
128. Pietras K, Östman A. Hallmarks of cancer: interactions with the tumor stroma. *Exp Cell Res.* 2010;316(8):1324–1331.
129. Mäkitie T, Summanen P, Tarkkanen A, Kivelä T. Tumor-infiltrating macrophages (CD68(+) cells) and prognosis in malignant uveal melanoma. *Invest Ophthalmol Vis Sci.* 2001;42(7):1414–1421.
130. Maat W, Ly LV, Jordanova ES, de Wolff-Rouendaal D, Schalij-Delfos NE, Jager MJ. Monosomy of chromosome 3 and an inflammatory phenotype occur together in uveal melanoma. *Invest Ophthalmol Vis Sci.* 2008;49(2):505–510.
131. Bronkhorst IHG, Ly LV, Jordanova ES, et al. Detection of M2-macrophages in uveal melanoma and relation with survival. *Invest Ophthalmol Vis Sci.* 2011;52(2):643–650.
132. Kato R, Haratani K, Hayashi H, et al. Nintedanib promotes antitumour immunity and shows antitumour activity in combination with PD-1 blockade in mice: potential role of cancer-associated fibroblasts. *Br J Cancer.* 2021;124(5):914–924.
133. Diazzi S, Baeri A, Fassy J, et al. Blockade of the pro-fibrotic reaction mediated by the miR-143/-145 cluster enhances the responses to targeted therapy in melanoma. *EMBO Mol Med.* 2022;14(3):e15295.
134. Fu Y, Saraswat A, Wei Z, et al. Development of dual ARV-825 and nintedanib-loaded PEGylated nano-liposomes for synergistic efficacy in vemurafnib-resistant melanoma. *Pharmaceutics.* 2021;13(7):1005.
135. Woodward JKL, Rennie IG, Burn JL, Sisley K. A potential role for TGFβ in the regulation of uveal melanoma adhesive interactions with the hepatic endothelium. *Invest Ophthalmol Vis Sci.* 2005;46(10):3473–3477.
136. Ballas MS, Chachoua A. Rationale for targeting VEGF, FGF, and PDGF for the treatment of NSCLC. *Onco Targets Ther.* 2011;4:43–58.
137. Toro MD, Gozzo L, Tracia L, et al. New therapeutic perspectives in the treatment of uveal melanoma: a systematic review. *Biomedicines.* 2021;9(10):1311.
138. Guenterberg KD, Grignol VP, Relekar KV, et al. A pilot study of bevacizumab and interferon-α2b in ocular melanoma. *Am J Clin Oncol.* 2011;34(1):87–91.
139. Bhatia S, Moon J, Margolin KA, et al. Phase II trial of sorafenib in combination with carboplatin and paclitaxel in patients with metastatic uveal melanoma: SWOG S0512. *PLoS One.* 2012;7(11):e48787.
140. Mahipal A, Tijani L, Chan K, Laudadio M, Mastrangelo MJ, Sato T. A pilot study of sunitinib malate in patients with metastatic uveal melanoma. *Melanoma Res.* 2012;22(6):440–446.
141. Mouriaux F, Servois V, Parienti JJ, et al. Sorafenib in metastatic uveal melanoma: efficacy, toxicity and health-related quality of life in a multicentre phase II study. *Br J Cancer.* 2016;115(1):20–24.
142. Daud A, Kluger HM, Kurzrock R, et al. Phase II randomised discontinuation trial of the MET/VEGF receptor inhibitor cabozantinib in metastatic melanoma. *Br J Cancer.* 2017;116(4):432–440.
143. Luke JJ, Olson DJ, Allred JB, et al. Randomized phase II trial and tumor mutational spectrum analysis from cabozantinib versus chemotherapy in metastatic uveal melanoma (Alliance A091201). *Clin Cancer Res.* 2020;26(4):804–811.
144. Semenza GL. HIF-1 and tumor progression: pathophysiology and therapeutics. *Trends Mol Med.* 2002;8(4 Suppl):S62–S67.
145. Cao Y, Cao R, Hedlund EM. R Regulation of tumor angiogenesis and metastasis by FGF and PDGF signaling pathways. *J Mol Med (Berl).* 2008;86(7):785–789.
146. Bergers G, Hanahan D. Modes of resistance to anti-angiogenic therapy. *Nat Rev Cancer.* 2008;8(8):592–603.
147. Ebos JML, Lee CR, Cruz-Munoz W, Bjarnason GA, Christensen JG, Kerbel RS. Accelerated metastasis after short-term treatment with a potent inhibitor of tumor angiogenesis. *Cancer Cell.* 2009;15(3):232–239.

148. Pàez-Ribes M, Allen E, Hudock J, et al. Antiangiogenic therapy elicits malignant progression of tumors to increased local invasion and distant metastasis. *Cancer Cell.* 2009;15(3):220–231.
149. Rapisarda A, Melillo G. Role of the hypoxic tumor microenvironment in the resistance to anti-angiogenic therapies. *Drug Resist Updat.* 2009;12(3):74–80.
150. Ferrara N. Pathways mediating VEGF-independent tumor angiogenesis. *Cytokine Growth Factor Rev.* 2010;21(1):21–26.
151. Franco M, Roswall P, Cortez E, Hanahan D, Pietras K. Pericytes promote endothelial cell survival through induction of autocrine VEGF-A signaling and Bcl-w expression. *Blood.* 2011;118(10):2906–2917.
152. Vasudev NS, Reynolds AR. Anti-angiogenic therapy for cancer: current progress, unresolved questions and future directions. *Angiogenesis.* 2014;17(3):471–494.
153. Serova M, Tijeras-Raballand A, Santos CD, et al. Everolimus affects vasculogenic mimicry in renal carcinoma resistant to sunitinib. *Oncotarget.* 2016;7(25):38467–38486.
154. Piperigkou Z, Manou D, Karamanou K, Theocharis AD. Strategies to target matrix metalloproteinases as therapeutic approach in cancer. *Methods Mol Biol.* 2018:1731:325–348
155. Ho D, Quake SR, McCabe ERB, et al. Enabling technologies for personalized and precision medicine. *Trends in Biotechnol.* 2020;38(5):497–518.